Supplement of

Coupling between surface ozone and leaf area index in a chemical transport model: Strength of feedback and implications for ozone air quality and vegetation health

Shan S. Zhou et al.

Correspondence to: A. P. K. Tai (amostai@cuhk.edu.hk)

Table S1: Plant functional types (PFTs) and their short names in CLM4.5.

No.	Plant functional type	Short name
1	Needleleaf evergreen tree – temperate	NET Temperate
2	Needleleaf evergreen tree – boreal	NET Boreal
3	Needleleaf deciduous tree – boreal	NDT Boreal
4	Broadleaf evergreen tree – tropical	BET Tropical
5	Broadleaf evergreen tree – temperate	BET Temperate
6	Broadleaf deciduous tree – tropical	BDT Tropical
7	Broadleaf deciduous tree – temperate	BDT Temperate
8	Broadleaf deciduous tree – boreal	BDT Boreal
9	Broadleaf evergreen shrub – temperate	BES Temperate
10	Broadleaf deciduous shrub – temperate	BDS Temperate
11	Broadleaf deciduous shrub – boreal	BDS Boreal
12	C_3 arctic grass	–
13	C_3 grass	–
14	C_4 grass	–
15	C_3 unmanaged rainfed crop	Rainfed Crop

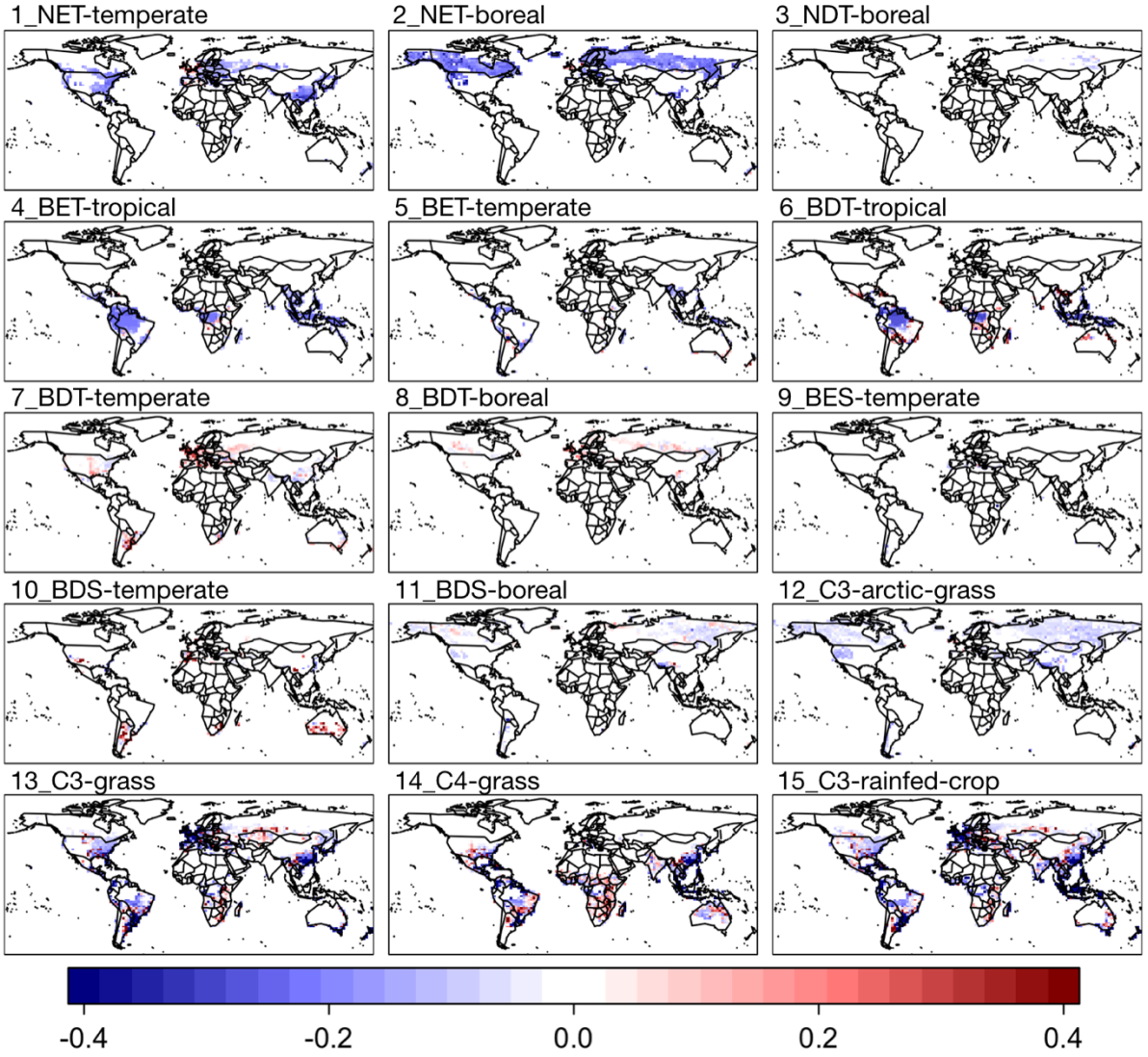

Figure S1: Fitted parameter, γ_∞ in Eq. (8) of the main text, minus one (i.e., $\gamma_\infty - 1$) for the 15 plant functional types (PFTs) represented in the Community Land Model (CLM4.5). The fitting is done for each month of the year, and here the annual average values are shown. Monthly values can be obtained by request.

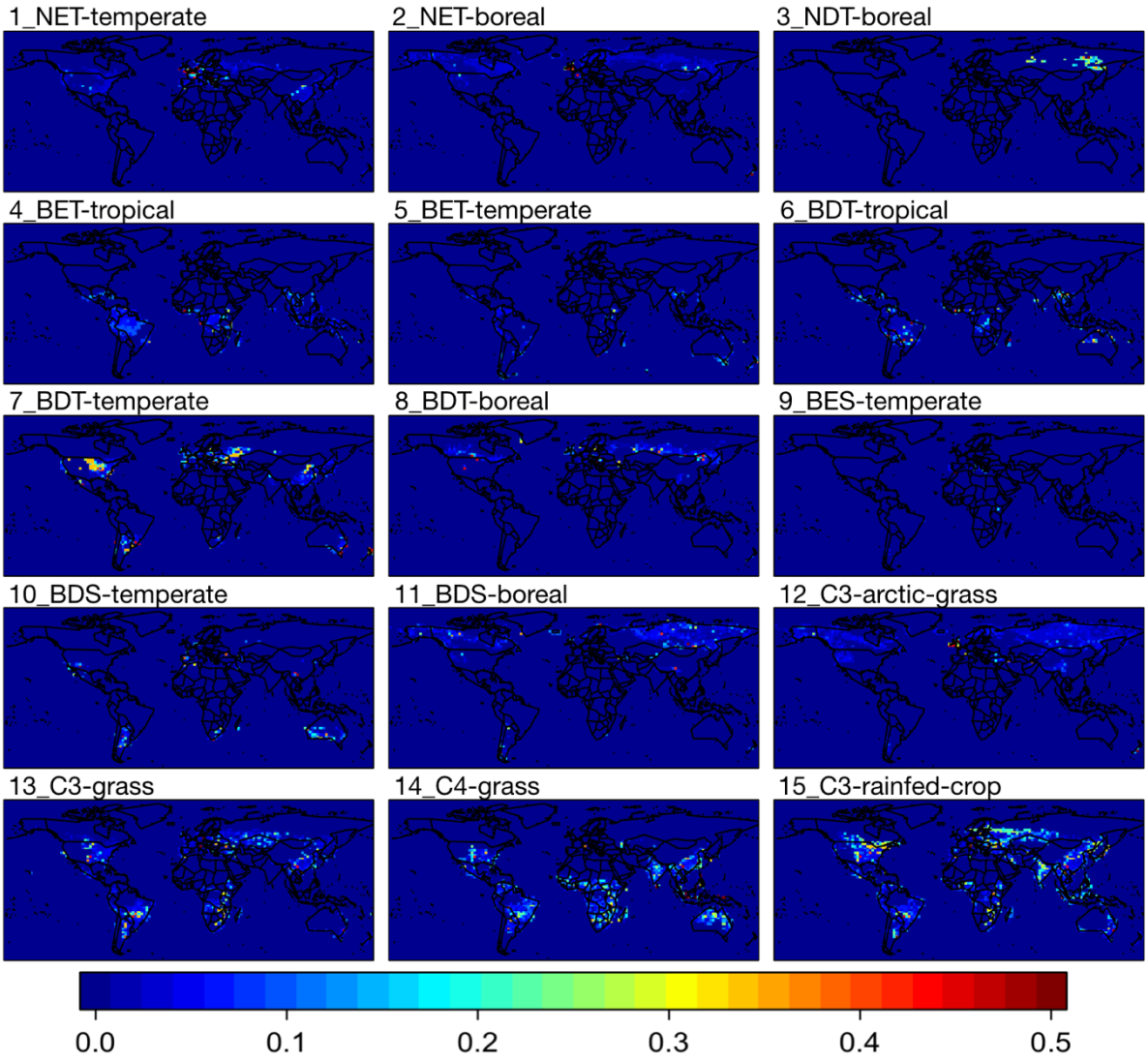

Figure S2: Fitted parameter, *k* in Eq. (8) of the main text, for the 15 plant functional types (PFTs) represented in the Community Land Model (CLM4.5). The fitting is done for each month of the year, and here the annual average values are shown. Monthly values can be obtained by request.

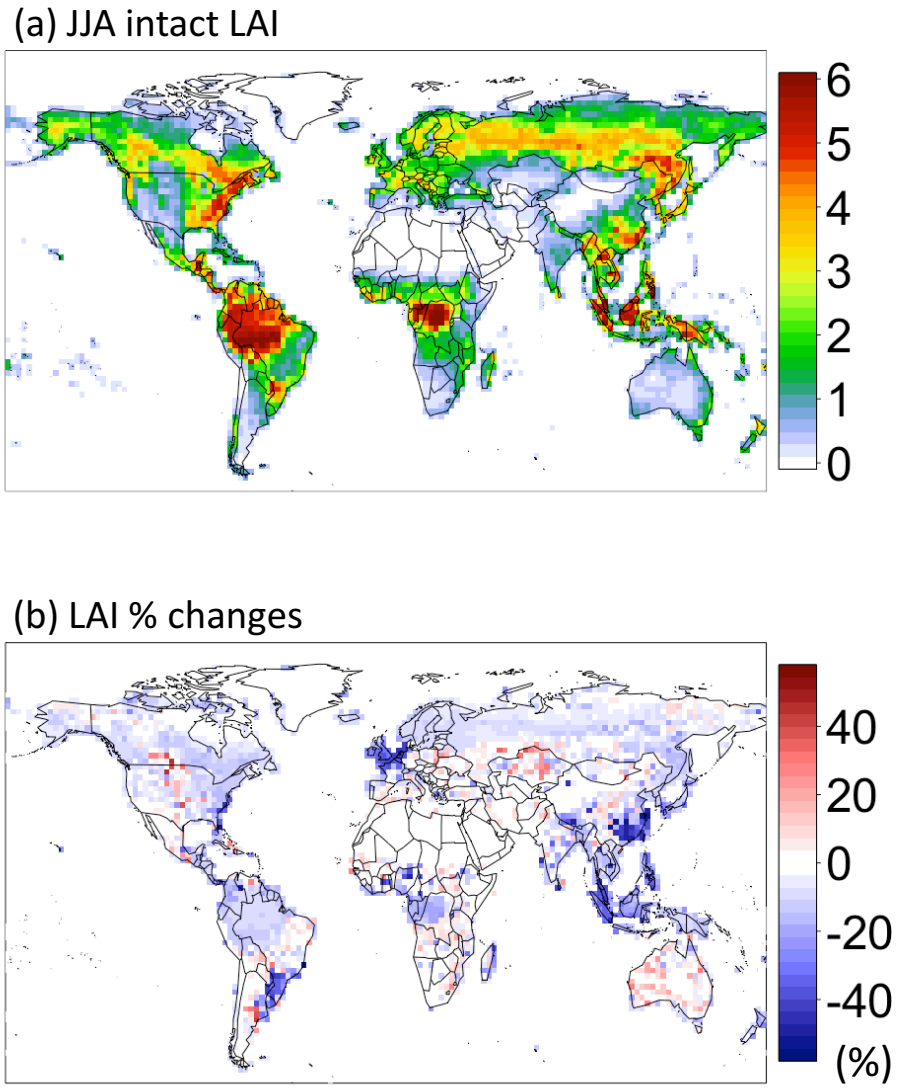

Figure S3: (a) Intact potential leaf area index (LAI) unaffected by ozone exposure in summer (JJA mean) as calculated by Eq. (9) in the main text; and (b) percentage changes in mean JJA LAI due to synchronous ozone-LAI coupling.

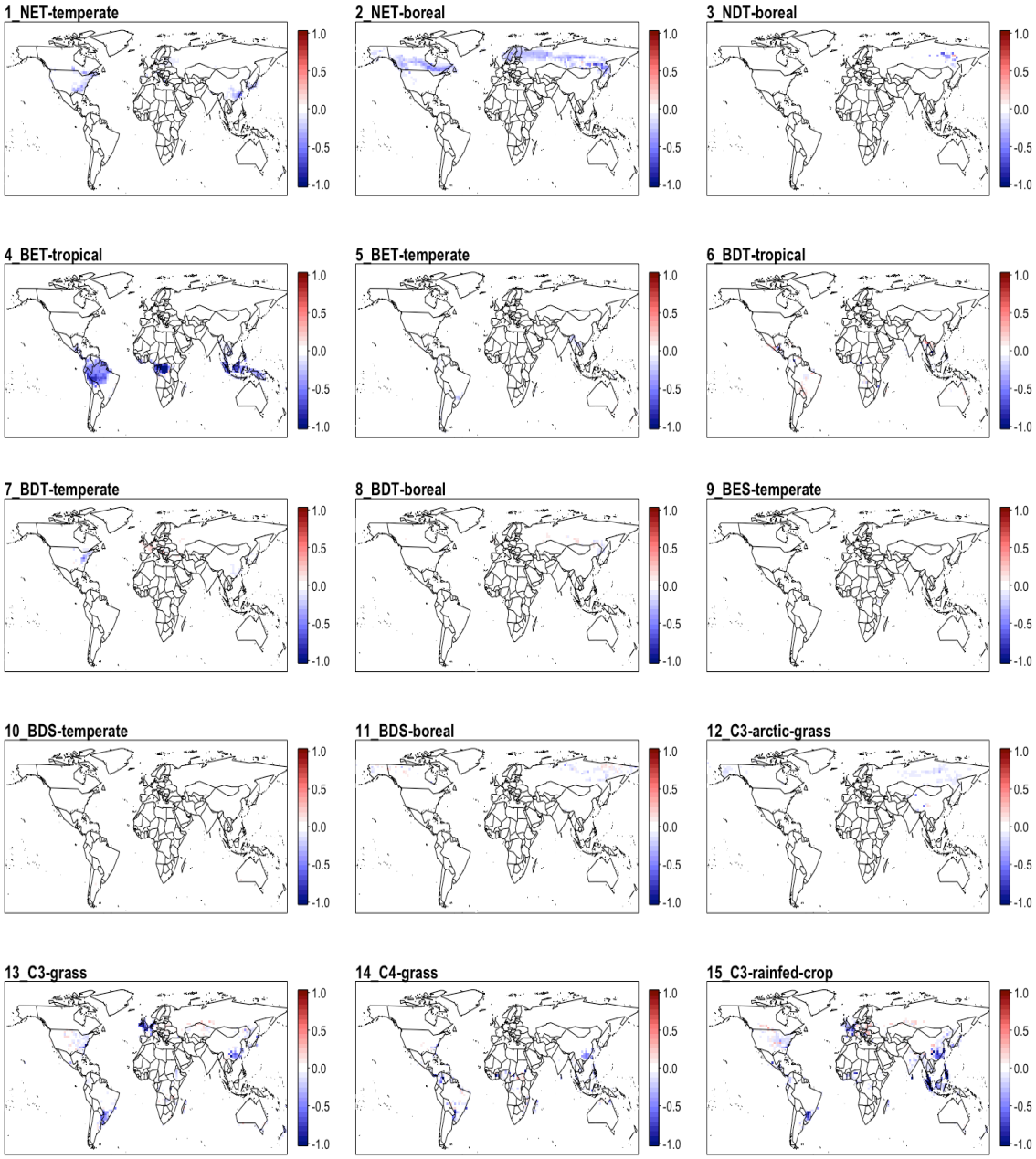

Figure S4: Changes in PFT-level leaf area index (LAI) between ozone-affected PFT-level LAI and intact potential PFT-level LAI unaffected by ozone in summer (acronyms are listed in Table S1).

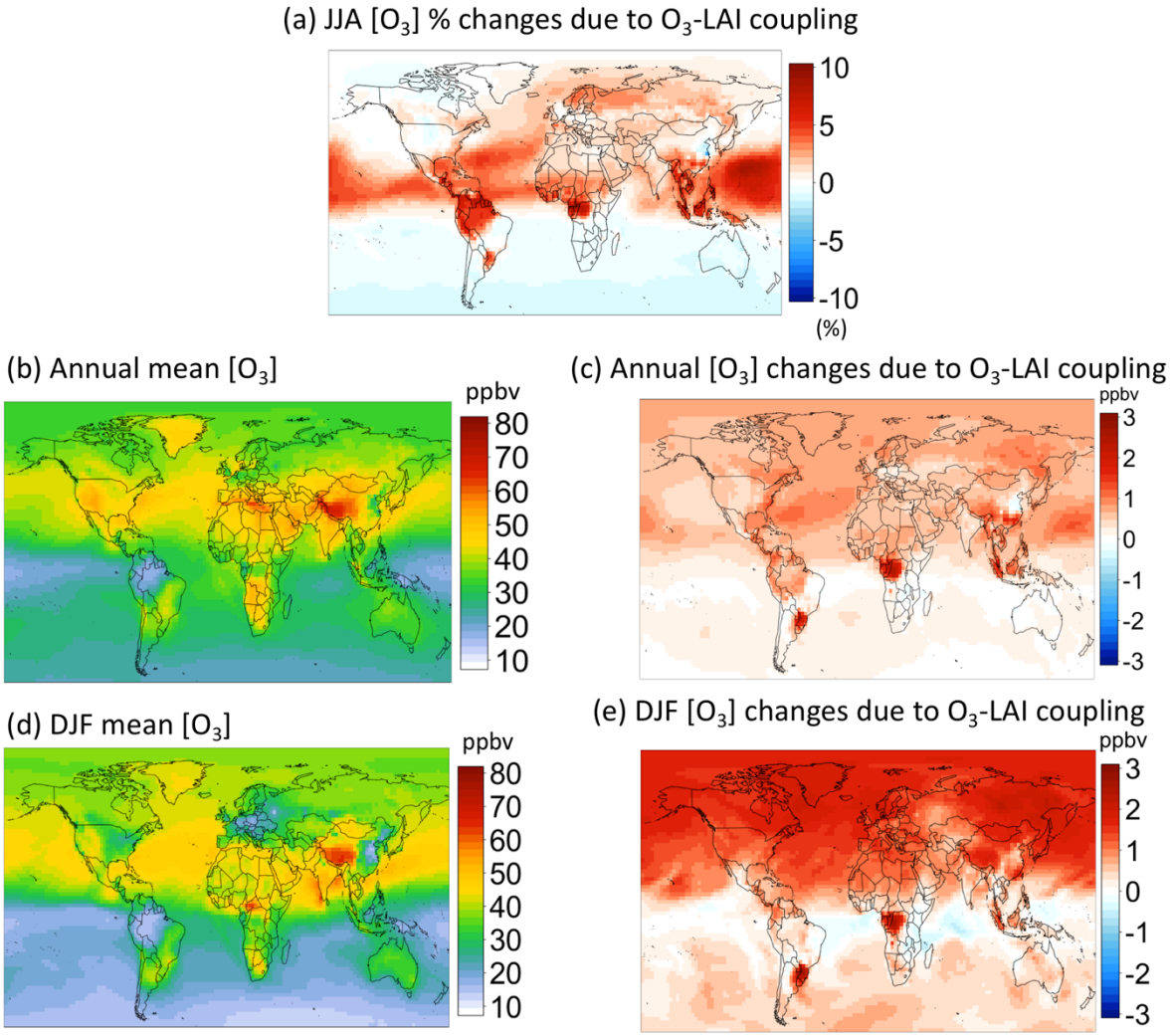

Figure S5: (a) Percentage changes in surface ozone concentration between the *[Affected LAI]* and *[Intact LAI]* case in summer (JJA mean); (b) and (d) Annual mean and boreal wintertime (DJF) mean surface ozone concentrations with ozone-affected leaf area index (LAI) from the *[Affected LAI]* case; and (c) and (e) differences in annual mean and DJF mean ozone concentrations between the *[Affected LAI]* and *[Intact LAI]* case (i.e., *[Affected LAI] – [Intact LAI]*).

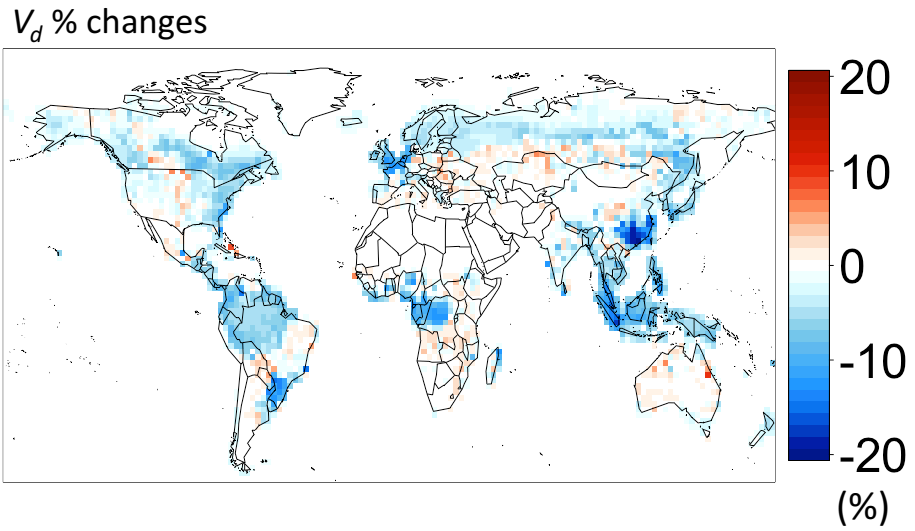

Figure S6: Percentage changes in summertime (JJA) ozone dry deposition velocity between the *[Affected LAI]* and *[Intact LAI]* case.

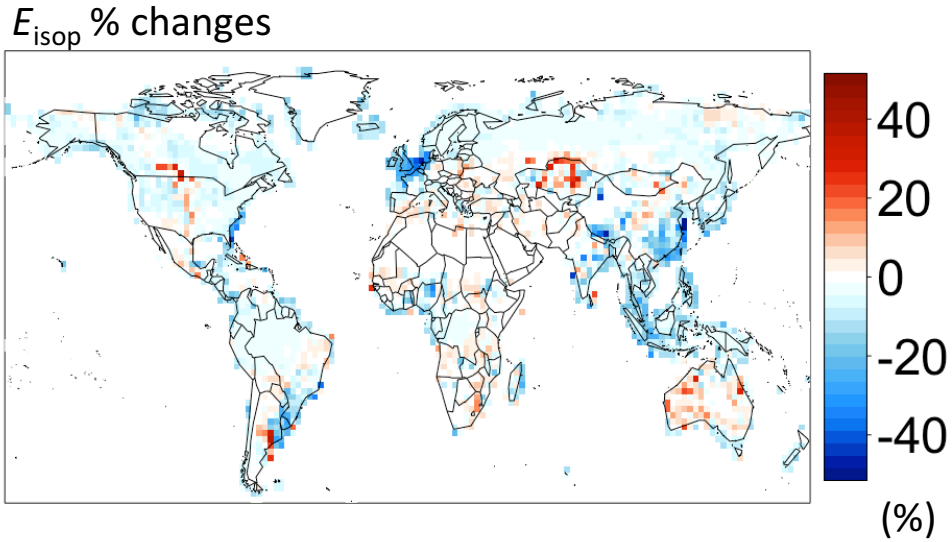

Figure S7: Percentage changes in isoprene emission rate between the *[Affected LAI]* case and *[Intact LAI]* case in summer (JJA mean).

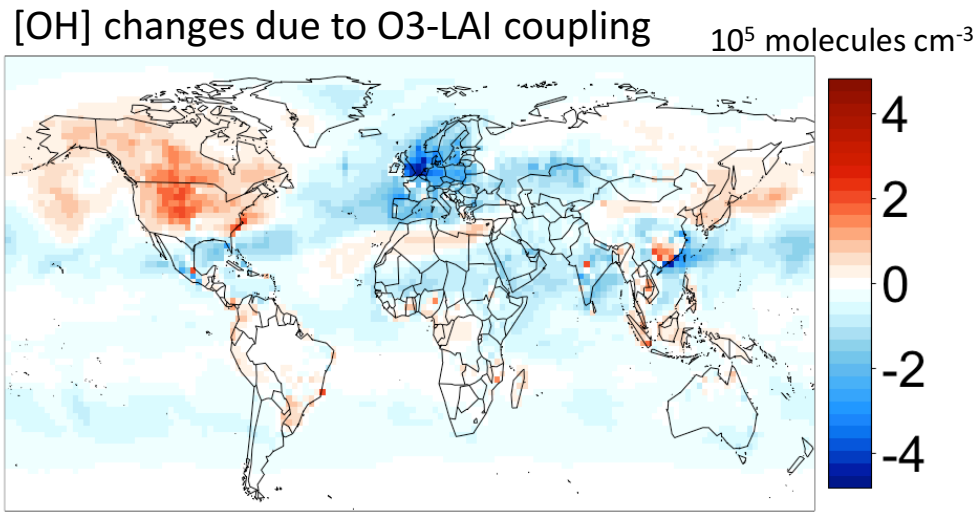

Figure S8: Absolute changes in OH concentration between the *[Affected LAI]* case and *[Intact LAI]* case in summer.

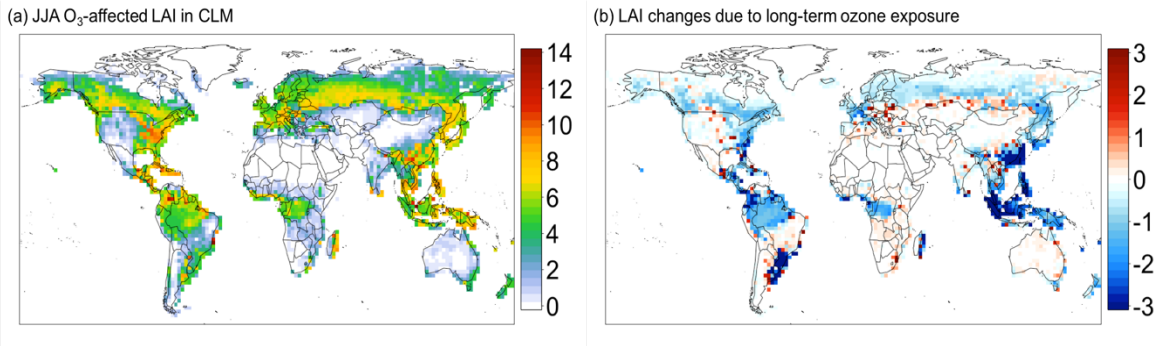

Figure S9: (a) Steady-state leaf area index (LAI) affected by long-term ozone exposure in summer (JJA mean) simulated by the Community Land Model (CLM); and (b) differences between ozone-affected LAI in (a) and intact LAI unaffected by ozone in the control case. Results are for asynchronous O_3-LAI coupling described in Sect. 5 of the main text.

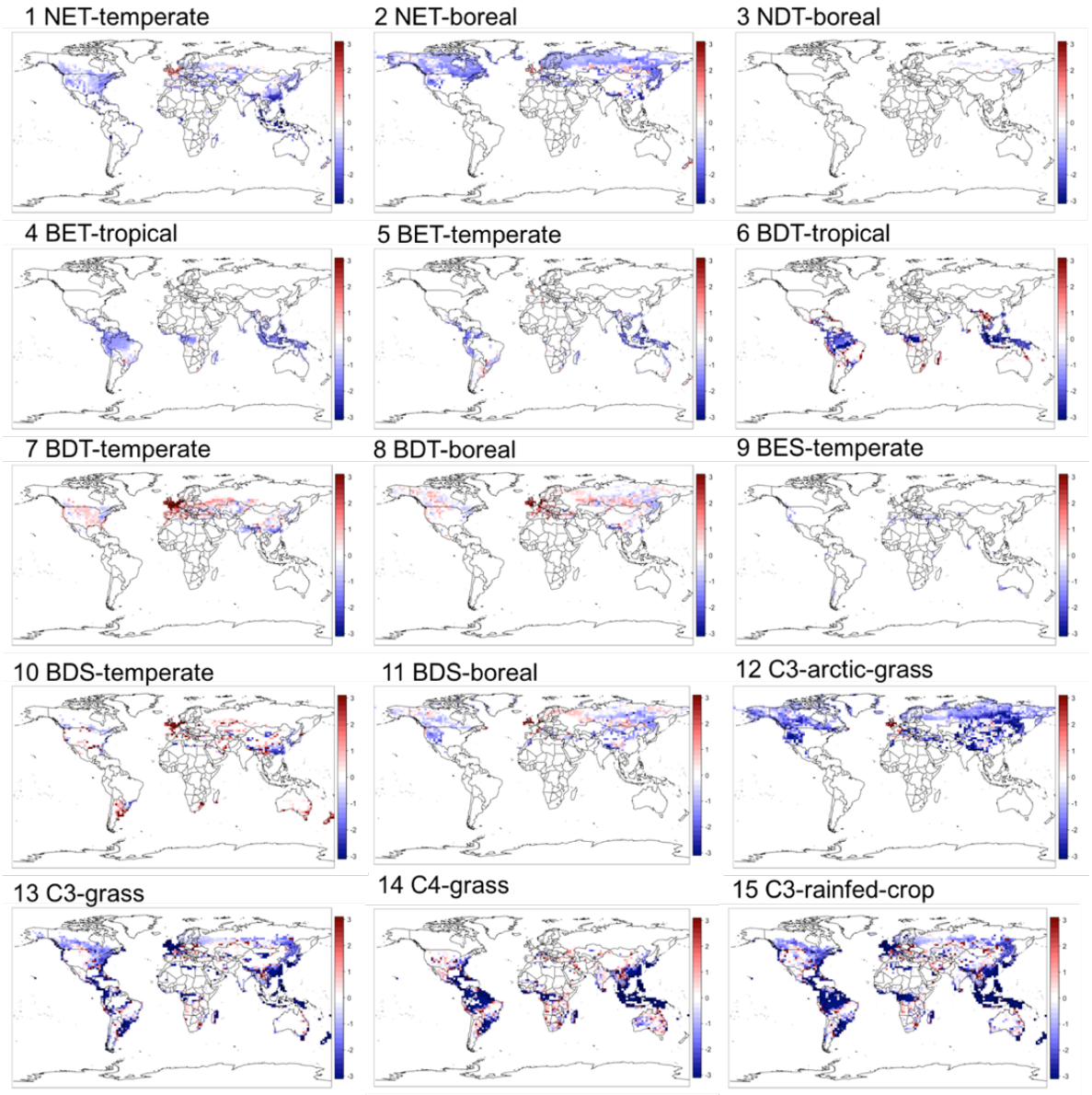

Figure S10: Changes in PFT-level leaf area index (LAI) between ozone-affected PFT-level LAI and intact PFT-level LAI unaffected by ozone simulated by CLM in summer. Results are for asynchronous O_3-LAI coupling described in Sect. 5 of the main text.

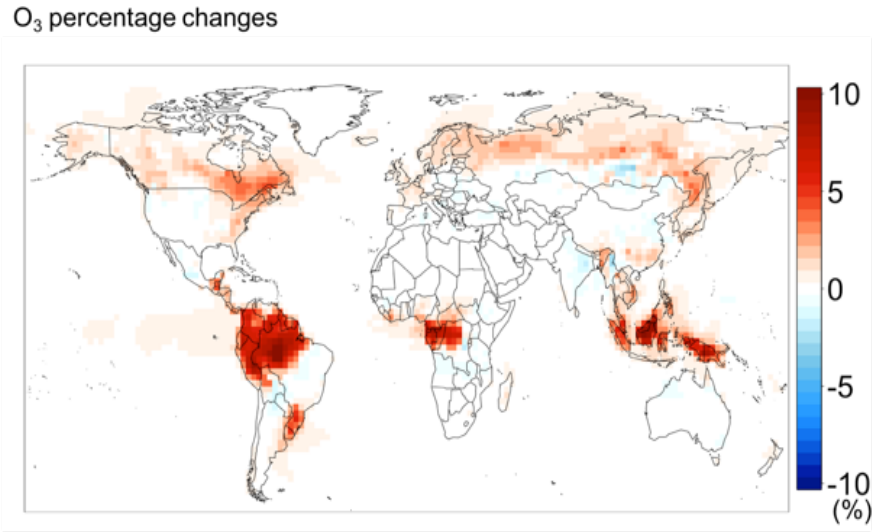

Figure S11: Percentage changes in surface ozone concentration between the *[Affected LAI]* and *[Intact LAI]* case in summer. Results are for asynchronous O_3-LAI coupling described in Sect. 5 of the main text.

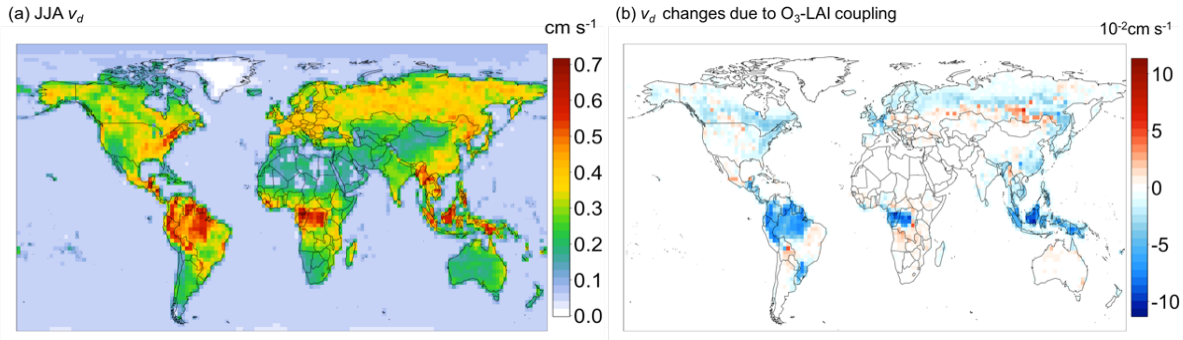

Figure S12: (a) Ozone dry deposition velocity (v_d) in summer (JJA mean) from the *[Affected LAI]* case; and (b) differences in ozone dry deposition velocity between the *[Affected LAI]* and *[Intact LAI]* case (i.e., *[Affected LAI] – [Intact LAI]*). Results are for asynchronous O_3-LAI coupling described in Sect. 5 of the main text.

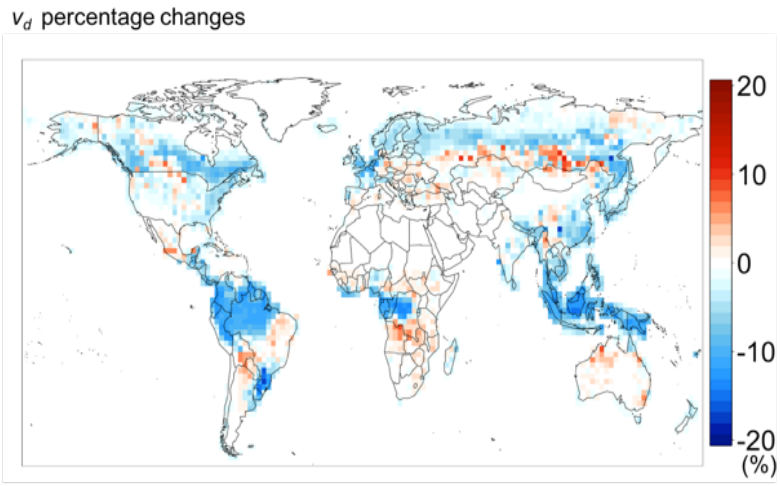

Figure S13: Percentage changes in summertime (JJA) ozone dry deposition velocity between the *[Affected LAI]* and *[Intact LAI]* case. Results are for asynchronous O_3-LAI coupling described in Sect. 5 of the main text.

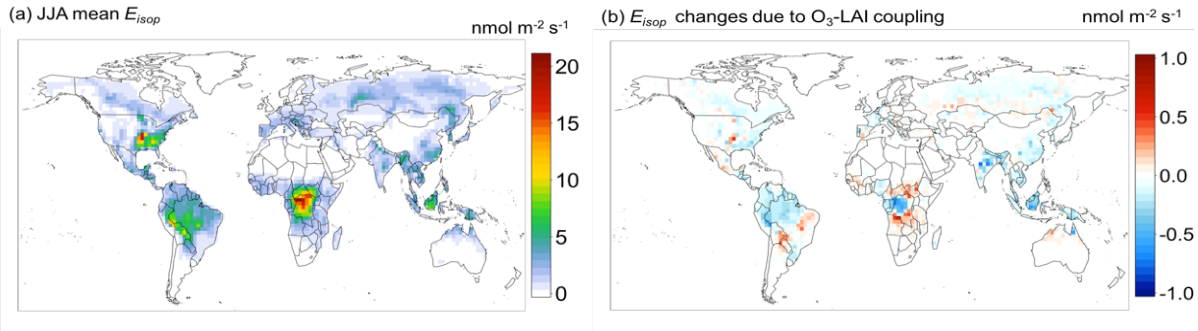

Figure S14: (a) Isoprene emission rate (E_{isop}) in summer (JJA mean) from the *[Affected LAI]* case; and (b) differences in isoprene emission rate between the *[Affected LAI]* and *[Intact LAI]* case (i.e., *[Affected LAI] – [Intact LAI]*). Results are for asynchronous O_3-LAI coupling described in Sect. 5 of the main text.

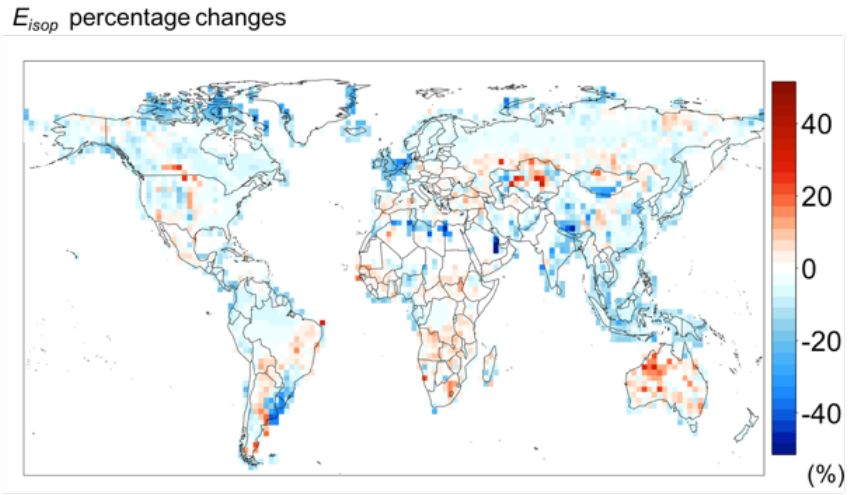

Figure S15: Percentage changes in isoprene emission rate between the *[Affected LAI]* and *[Intact LAI]* case in summer. Results are for asynchronous O_3-LAI coupling described in Sect. 5 of the main text.

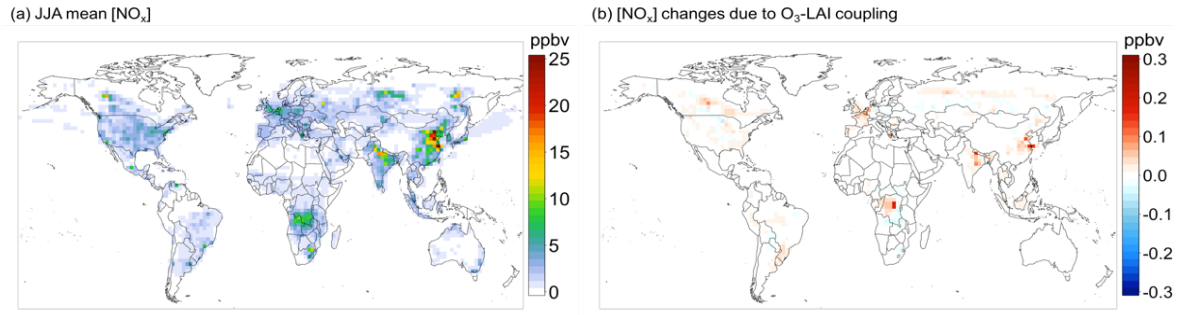

Figure S16: (a) Surface NO_x concentration in summer (JJA mean) from the *[Affected LAI]* case; and (b) differences in NO_x concentration between the *[Affected LAI]* and *[Intact LAI]* case (i.e., *[Affected LAI] – [Intact LAI]*). Results are for asynchronous O_3-LAI coupling described in Sect. 5 of the main text.